Roles of Cannabinoid Receptors Type 1 and 2 on the Retinal Function of Adult Mice

Bruno Cécyre,[1,2] Nawal Zabouri,[1,2] Frédéric Huppé-Gourgues,[3] Jean-François Bouchard,[2] and Christian Casanova[1]

[1]Laboratoire des neurosciences de la vision, École d'optométrie, Université de Montréal, Québec, Canada
[2]Laboratoire de neuropharmacologie, École d'optométrie, Université de Montréal, Québec, Canada
[3]Laboratoire de neurobiologie de la cognition visuelle, École d'optométrie, Université de Montréal, Montréal, Québec, Canada

Correspondence: Jean-François Bouchard, Laboratoire de neuropharmacologie, École d'optométrie, Université de Montréal, C.P. 6128 Succursale Centre-Ville, Montréal, QC, Canada H3C 3J7; jean-francois.bouchard@umontreal.ca.

BC and NZ contributed equally to the work presented here and should therefore be regarded as equivalent authors.

Submitted: May 31, 2013
Accepted: November 1, 2013

Citation: Cécyre B, Zabouri N, Huppé-Gourgues F, Bouchard J-F, Casanova C. Roles of cannabinoid receptors type 1 and 2 on the retinal function of adult mice. *Invest Ophthalmol Vis Sci.* 2013;54:8079–8090. DOI:10.1167/iovs.13-12514

Purpose. Endocannabinoids are important modulators of synaptic transmission and plasticity throughout the central nervous system. The cannabinoid receptor type 1 (CB1R) is extensively expressed in the adult retina of rodents, while CB2R mRNA and protein expression have been only recently demonstrated in retinal tissue. The activation of cannabinoid receptors modulates neurotransmitter release from photoreceptors and could also affect bipolar cell synaptic release. However, the impact of CB1R and CB2R on the retinal function as a whole is currently unknown.

Methods. In the present study, we investigated the function of cannabinoid receptors in the retina by recording electroretinographic responses (ERGs) from mice lacking either CB1 or CB2 receptors (*cnr1*$^{-/-}$ and *cnr2*$^{-/-}$, respectively). We also documented the precise distribution of CB2R by immunohistochemistry.

Results. Our results showed that CB2R is localized in cone and rod photoreceptors, horizontal cells, some amacrine cells, and bipolar and ganglion cells. In scotopic conditions, the amplitudes of the a-wave of the ERG were increased in *cnr2*$^{-/-}$ mice, while they remained unchanged in *cnr1*$^{-/-}$ mice. The analysis of the velocity-time profile of the a-wave revealed that the increased amplitude was due to a slower deceleration rather than an increase in acceleration of the waveform. Under photopic conditions, b-wave amplitudes of *cnr2*$^{-/-}$ mice required more light adaptation time to reach stable values. No effects were observed in *cnr1*$^{-/-}$ mice.

Conclusions. The data indicated that CB2R is likely to be involved in shaping retinal responses to light and suggest that CB1 and CB2 receptors could have different roles in visual processing.

Keywords: endocannabinoids, CB1R, CB2R, ERG, retina

Cannabinoids (CBs) are the principal psychoactive components of marijuana plant (*Cannabis sativa*). The endocannabinoid (eCB) system is involved in a variety of neurobiological functions such as signal processing, nociception, learning and memory, and motor coordination. Endocannabinoids are generally associated with the modulation of neuronal transmission and, more recently, with developmental processes. In the last decade, several studies have shown that CB receptors (CBRs) are present in the retina of most mammals including humans,[1] suggesting that the eCB system could be involved in some aspects of visual processing.

The cannabinoid receptor type 1 (CB1R) is ubiquitously expressed in the nervous system. In the retina, its presence has been shown in several species, ranging from fishes to primates[2–9] (see Yazulla[10] for review). Briefly, CB1R is present in cones, horizontal cells, some bipolar cells, and amacrine and ganglion cells. Patch-clamp studies have demonstrated that CB1R activation differentially modulates ion channels in photoreceptors and glutamate synaptic release.[11–13] In bipolar cells, CB1R activation inhibits calcium[2] and potassium rectifying[14] currents. Functionally, these effects could lead to a decreased synaptic release and changes in the temporal aspects of bipolar cells' response. In addition, CB1R activation can also modulate gamma-aminobutyric acid (GABA)ergic release from amacrine cells[8] and inhibit high-voltage–activated calcium channel in cultured ganglion cells, which impacts the cells' excitability.[9] It is not known how the reported effects are reflected at the global functional level.

Although cannabinoid receptor type 2 (CB2R) expression in neurons remains controversial, several authors have reported a sparse expression in neurons in several structures such as the cerebellum, brainstem, hippocampus, and prefrontal cortex (see Atwood and Mackie[15] for review). Only two studies[16,17] have demonstrated the presence of CB2R in the rodent retina. From its mRNA distribution, Lu et al.[16] have localized CB2R in photoreceptors, inner nuclear layer, and ganglion cell layer in the adult rat retina. While this study provides valuable information, the results do not confirm the presence of CB2R in the retina, since G protein–coupled receptor mRNA and protein expression at the cell surface do not necessarily correlate.[18] Using cells' morphology and position, CB2R protein has been more precisely localized by Lopez et al.[17] in the same animal model: it was found in the inner segment of photoreceptors and in horizontal, amacrine, and ganglion cells.

Table 1. Antibodies Used in This Study

Antibody	Target	Immunogen	Dilution	Host	Provenance
CB2R	Cannabinoid receptor type 2	N-terminus 14 aa of human CB2R (20–33 residues)	I, 1:200 W, 1:2000	Rabbit	101550; Cayman Chemical, Ann Arbor, MI
CB1R	Cannabinoid receptor type 1	N-terminus 77 aa of rat CB1R (1–77 residues)	W, 1:1000	Rabbit	C1233; Sigma-Aldrich, Oakville, ON, Canada
NAPE-PLD	N-acyl phosphatidyethanolamine phospholipase D	N-terminus 13 aa of mouse NAPE-PLD (9–21 residues)	W, 1:500	Rabbit	NB110-80070; Novus Biologicals, Oakville, ON, Canada
DAGLα	Diacylglycerol lipase α	C-terminus 42 aa of mouse DAGLα (1003–1044 residues)	W, 1:200	Rabbit	DGLa-Rb-Af380; Frontier Institute, Ishikari, Hokkaido, Japan
FAAH	Fatty acid amide hydrolase	C-terminus 19 aa rat FAAH (561–579 residues)	W, 1:3000	Rabbit	101600; Cayman Chemical
MGL	Monoacylglycerol lipase	N-terminus 35 aa of mouse MGL (1–35 residues)	W, 1:200	Rabbit	MGL-Rb-Af200; Frontier Institute
GAPDH	Loading control	The full-length rabbit muscle GAPDH protein	W, 1:20,000	Mouse	G8795; Sigma-Aldrich
Mouse cone-arrestin (LUMIj)	Cone photoreceptors	C-terminus 13 aa of the mCAR protein (369–381 residues)	I, 1:1000	Rabbit	Cheryl M. Craft, Mary D. Allen Laboratory for Vision Research, Doheny Eye Institute, USC, Los Angeles, CA
Recoverin	Rod photoreceptors, and ON and OFF cone bipolar cells	The full-length recombinant human recoverin	I, 1:2000	Rabbit	AB5585; EMD Milipore Corporation, Billerica, MA
Calbindin (D-28K)	Horizontal and amacrine cells	Recombinant rat calbindin D-28K full length	I, 1:1000	Rabbit	CB-38a; Swant, Marly, Switzerland
PKC (clone H7)	Rod bipolar cells	C-terminus 28 aa of human protein (645–672 residues)	I, 1:500	Mouse	Sc-8393; Santa Cruz Biotechnology, Santa Cruz, CA
Syntaxin (clone HPC1)	Amacrine cells	Synaptosomal plasma fraction of rat hippocampus	I, 1:500	Mouse	S0664; Sigma-Aldrich
Brn-3a (clone 5A3.2)	Ganglion cells	Amino acids 186–224 of Brn-3a fused to the T7 gene 10 protein	I, 1:100	Mouse	MAB1585; EMD Millipore Corporation
Glutamine synthetase (GS, clone GS-6)	Müller cells	The full protein purified from sheep brain	I, 1:3000	Mouse	MAB302; EMD Millipore Corporation

aa, amino acids; I, immunohistochemistry; W, Western blot.

However, the CB2R antibody used by these authors was not fully characterized. Thus, the exact localization of CB2R in retinal cells remains an open question. To our knowledge, no studies have investigated the effect of CB2R activation at the retinal level.

The objective of this study was to evaluate the roles of CBRs in the retinal function in a mammalian in vivo model. To achieve this goal, electroretinograms (ERGs, representing the global evoked response of the retina) of mice lacking CB1 or CB2 receptors (*cnr1*$^{-/-}$ and *cnr2*$^{-/-}$, respectively) and their wild-type (WT) controls were compared under different light conditions. Given that the exact expression of pattern CB2R in the retina remains debatable, the presence of CB2R in the mice retina was confirmed and precisely assessed with a specific CB2R antibody and specific retinal markers. Our results indicate that CB2R is largely expressed by retinal neurons of mice and suggest that this receptor is likely to play a greater role in retinal processing than CB1R.

Methods

Animals

All procedures were performed in accordance with the guidelines from the Canadian Council on Animal Care and the ARVO Statement for the Use of Animals in Ophthalmic and Vision Research, and were approved by the Ethics Committee on Animal Research of the Université de Montréal. The *cnr1*$^{-/-}$ and *cnr2*$^{-/-}$ transgenic mice were obtained from Beat Lutz (Institute of Physiological Chemistry and Pathobiochemistry, University of Mainz, Germany) and Jackson Laboratory (Bar Harbor, ME), respectively. The *cnr1*$^{-/-}$ and *cnr2*$^{-/-}$ mice were on a C57BL/6N and C57BL/6J genetic background, respectively. Both transgenic mice were compared to background and age-matched WT controls from separate colonies. All animals were maintained in-house, under a 12-hour dark/light cycle. Male and female adult mice (3–4 months old) were used for the experiments.

Tissue Preparation

Mice were euthanized by an overdose of isoflurane. One eye was immediately removed for Western blot analysis. The retina was dissected on ice, promptly frozen, and kept at –80°C until further processing. Simultaneously, a transcardiac perfusion was conducted with phosphate-buffered 0.9% saline (PBS; 0.1 M, pH 7.4), followed by phosphate-buffered 4% paraformaldehyde (PFA), until the head was lightly fixed. The nasal part of the second eye was marked with a suture and removed. Two small holes were made in the cornea before a first postfixation in 4% PFA for a period of 30 minutes. The cornea and lens were removed and the eyecups were postfixed for 30 minutes in 4% PFA. The eyecups were then washed in PBS, cryoprotected in 30% sucrose overnight, embedded in Neg 50 tissue Embedding Media (Fisher Scientific, Ottawa, ON, Canada), flash-frozen and kept at –80°C. Sections (14 μm thick) were cut with a cryostat (Leica Microsystems, Concord, ON, Canada) and placed on gelatin/chromium-coated slides.

Western Blot

Retinas were homogenized in RIPA buffer (150 mM NaCl, 20 mM Tris, pH 8.0, 1% NP-40, 0.1% SDS, 1 mM EDTA), supplemented with a protease inhibitor mixture (aprotinin, leupeptin, pepstatin [1 μg/mL] and phenylmethylsulfonyl fluoride [0.2 mg/mL]; Roche Applied Science, Laval, QC, Canada). Thirty micrograms of protein per sample of the homogenate were resolved by electrophoresis on a 10% SDS-polyacrylamide gel, transferred onto a nitrocellulose membrane, blocked with 5% skim milk, and incubated overnight with antibodies directed against CB2R, CB1R, N-acyl phosphatidyethanolamine phospholipase D (NAPE-PLD), diacylglycerol lipase α (DAGLα), fatty acid amide hydrolase (FAAH), monoacylglycerol lipase (MGL), or glyceraldehyde 3-phosphate dehydrogenase (GAPDH), the latter serving as a loading control. The blots were exposed to the appropriate horseradish peroxidase–coupled secondary antibodies (Jackson Immunoresearch Laboratories, West Grove, PA). Detection was carried out by using homemade ECL Western blot detection reagents (final concentrations: 2.5 mM luminol, 0.4 mM p-coumaric acid, 0.1 M Tris-HCl pH 8.5, 0.018% H_2O_2).

Immunohistochemistry

Frozen sections were washed in PBS, postfixed for 10 minutes in cold acetone, washed, and then blocked in 1% bovine serum albumin, bovine gelatin, and 0.5% Triton X-100 in PBS for 1 hour. Some sections from WT animals were incubated overnight in rabbit anti-CB2R solution with an antibody against various retinal markers. In addition, sections from the three genotypes were incubated with retinal markers (see Table 1) to compare the distribution and morphology of retinal cells. The sections were then washed in PBS, blocked for 30 minutes, incubated for 1 hour with Alexa Fluor 647 donkey anti-rabbit for CB2R and Alexa Fluor 488 donkey anti-rabbit or Alexa Fluor 488 donkey anti-mouse for cell type markers (Molecular Probes, Eugene, OR). After washes, the sections were mounted with homemade PVA-Dabco mounting medium. The CB2R/recoverin, CB2R/cone-arrestin,[19–21] and CB2R/calbindin combinations required serial incubations, as the retinal marker host was rabbit, as previously performed on retinal tissues.[6] The dilution factors, the immunogens, and provenance of the antibodies are provided in Table 1.

Antibody Characterization

The CB2R antibody has been characterized in mice renal tissue[22]; consequently, we tested its specificity in the mice retina by Western blot and immunohistochemistry. The anti-CB2R reacted with a robust band at 45 kDa (Fig. 1A), which was absent with the addition of the immunizing peptide. No unspecific signal could be observed on retinal sections when CB2R antibody was preincubated with its immunizing peptide (Fig. 1B). Moreover, no unspecific signal was visible in the *cnr2*$^{-/-}$ mice (Fig. 1C), whereas the CB2R staining in the WT mouse yielded a strong signal in the retina (Fig. 1D). It should be noted that this antibody showed inconsistent results from one lot to another. These results display the specificity of lot No. 0424681-1.

Confocal Microscopy

Images of the central retina (within 200 μm of the optic nerve head) were taken with a laser scanning confocal microscope (TCS SP2; Leica Microsystems), with an ×40 oil immersion objective. Image stacks (1024 × 1024 pixels × 0.5 μm per stack) were captured by using the Leica confocal (LCS) software (version 2.6.1; Leica Microsystems). Offline processing was done with the Fiji software (version 1.47g; www.fiji.sc).[23] The stack images were taken sequentially to ensure no "bleed-through" between channels. Gaussian noise from images was partially removed by using the PureDenoise plugin for Fiji[24] and stacks were collapsed to projection images.

Investigative Ophthalmology & Visual Science

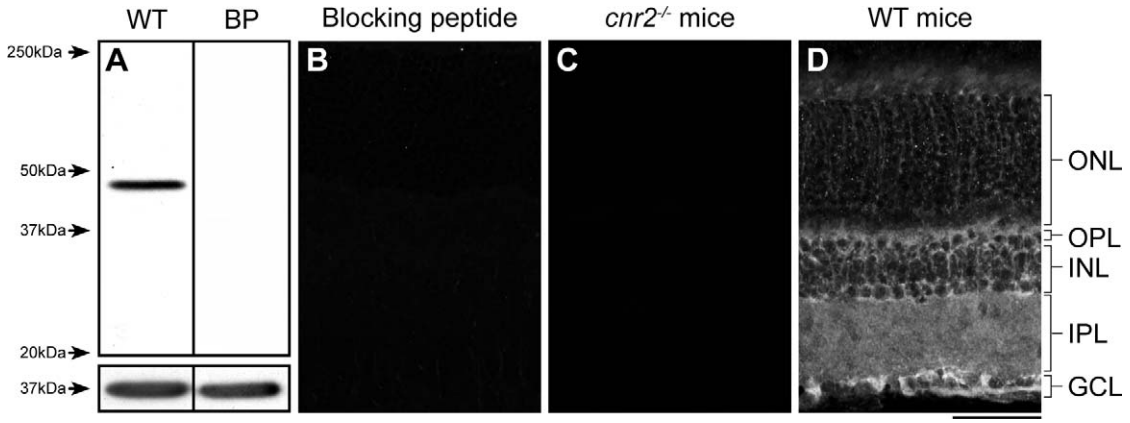

Figure 1. Characterization of an antibody directed against CB2R in adult mice retina. Immunoblots of CB2R immunoreactivity in a WT mouse retina and in presence of its blocking peptide (BP) (**A**). Specific band was seen at around 45 kDa in WT group only. GAPDH was used as a loading control. CB2R immunoreactivity in the retina of a WT mouse in presence of its appropriate BP (**B**), in *cnr2*$^{-/-}$ mice (**C**), and in WT mouse (**D**). All images were taken with identical microscopy settings. *Scale bar*: 50 μm.

Electroretinography

The ERG recordings were performed as previously reported.[25] Briefly, after an overnight dark adaptation (at least 12 hours of complete darkness), mice were anesthetized (ketamine 85 mg/kg, xylazine 5 mg/kg). Pupils were dilated with a drop of 1% cyclopentolate hydrochloride. The mice were then positioned in a Ganzfeld dome that housed a photostimulator (PS33plus; Grass Instruments, Middleton, WI). The ERGs were recorded with a silver wire electrode inserted in a custom-made corneal lens adapted for mice.[26] Reference and ground electrodes (E2 subdermal electrode; Grass Instruments) were inserted subcutaneously at the base of the head and in the tail. Broadband ERGs (bandwidth, 1–1000 Hz; 10,000×) (P511; Grass Instruments) and oscillatory potentials (bandwidth, 100–1000 Hz; 50,000×) were recorded simultaneously. Signals were fed to an analog-digital interface (1401; CED, Cambridge, UK) and were acquired by using the software Signal (v.3.01x; CED). Scotopic luminance-response functions were obtained in response to progressively brighter stimuli spanning a 3.97 log-unit range (interstimulus interval: 10 seconds; average: 5 flashes; luminance interval −2.3 to 1.67 log scot cd-s/m^2). The photopic (cone-mediated) signal was recorded thereafter: Electroretinograms were recorded every 5 minutes for 20 minutes under a photopic background of 30 cd/m^2 (flash luminance: 1.36 log photo cd-s/m^2; interstimulus interval: 1 second, averaged over 20 flashes).

Analysis

Analysis of the ERG waveforms was performed according to standard practice.[27] The amplitude of the a-wave was measured from baseline to the most negative trough, whereas the b-wave amplitude was measured from the trough of the a-wave to the highest positive peak of the retinal response. The kinetics of the a-wave was also analyzed by calculating the velocity-time profile at a photoreceptor saturating luminance[28] computed as the derivative of the waveform. All the points of the a-wave were taken into account. The last point of the waveform was set as the first derivative value equal or superior to 0. Implicit times were measured from flash onset to the peak of the waves. Scotopic luminance-response function curves were obtained by plotting the amplitude of the b-wave against the luminance of the flash used to evoke each response.

The mixed V_{max} referred to the highest evoked amplitude of the b-wave. The amplitude of oscillatory potentials (OPs) was measured and reported as the sum of the OPs ($OP_{1/2} + OP_3 + OP_4 + OP_5$ in scotopic conditions and $OP_1 + OP_2 + OP_3$ in photopic conditions). In a randomly chosen subgroup of animals, a fast Fourier transform analysis was performed with Matlab (The Mathworks, Nattick, MA) to confirm that no changes occurred in the power/frequency distribution of the ERG waveform. Statistical analysis was performed by using repeated measures ANOVA followed by one-way ANOVA and Dunnett post hoc test (SPSS 20; IBM, Somers, NY).

Quantification of Retinal Layer Thickness

Frozen sections were washed in PBS, and their nuclei were labeled with Sytox Green Nucleic Acid Stain (1:100,000; Molecular Probes) for 1 hour. The thickness of each retinal layer was measured at ×40 magnification, including the outer nuclear layer (ONL), the outer plexiform layer (OPL), the inner nuclear layer (INL), the inner plexiform layer (IPL), and the ganglion cell layer (GCL). The thickness of each layer was measured with LCS software (version 2.6.1; Leica Microsystems) and was normalized with respect to the total thickness of the retina to correct for local and interanimal variations. Statistical analysis was performed by using one-way ANOVA.

Results

Localization of CB2R in the Mice Retina

Our data indicated that the CB2 receptor is widely distributed in the retina. CB2R immunoreactivity in the photoreceptor layer was mostly found in cones, but rods were also labeled. CB2R was present in the outer and inner segments, in the cell body, but not in the pedicles of cones (Fig. 2A). It was also expressed in the inner and outer segments and cell body of rod photoreceptors (Fig. 2B).

Horizontal cells showed expression of CB2R at the membrane of the soma and in their dendrites (Fig. 2C). Both rod and cone bipolar cells were CB2R immunoreactive at the membrane of the soma (Figs. 2D, 2E). Rod bipolar cells also expressed CB2R at their dendrites and axons (Figs. 2E, 2F).

Investigative Ophthalmology & Visual Science

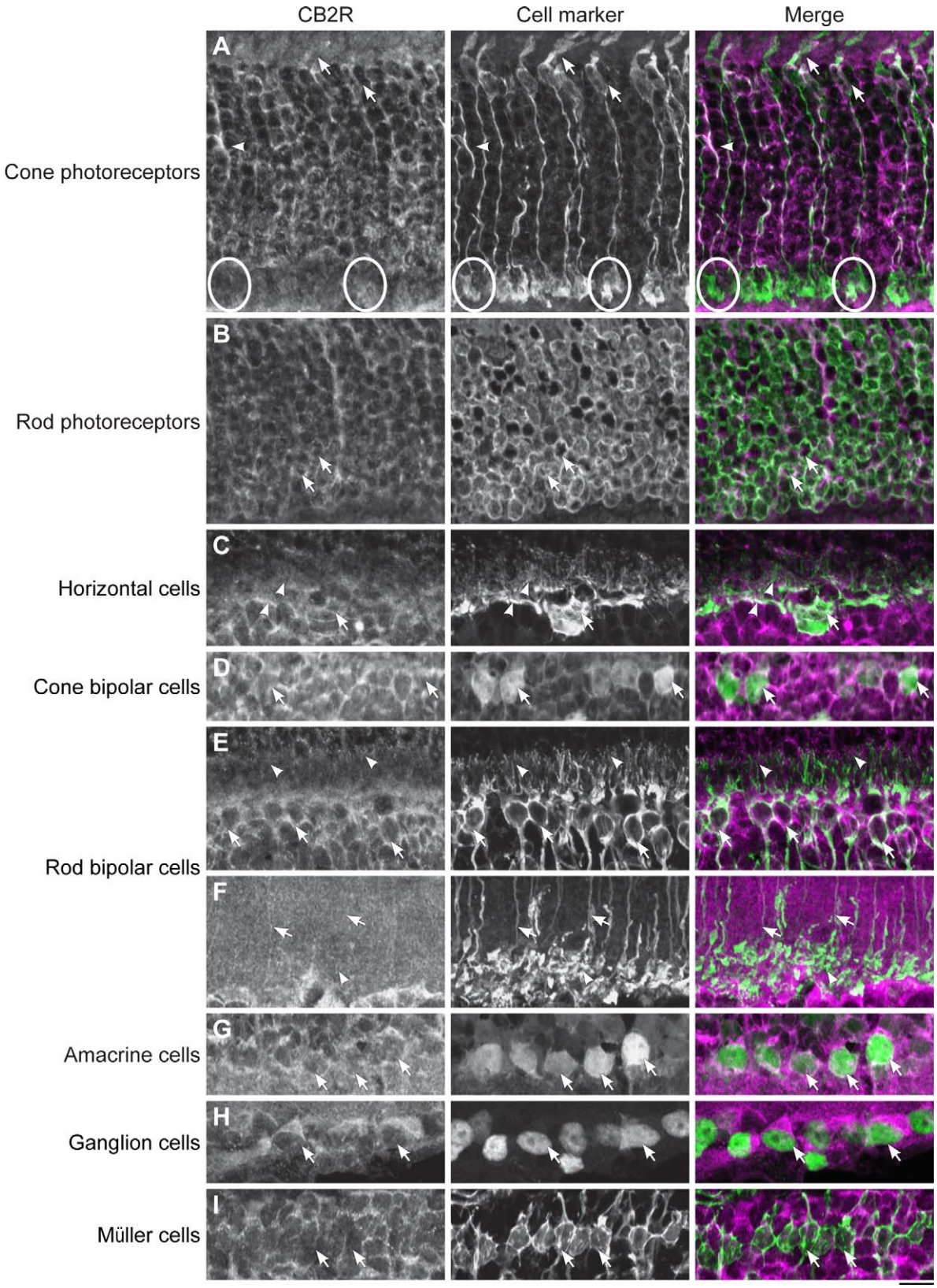

Figure 2. Double-label immunofluorescence illustrating colocalization of CB2R throughout the mouse retina. CB2R (*magenta*) is present in inner (*arrowheads*) and outer (*arrows*) segments of cones (mouse cone-arrestin), but not in pedicles (*circles*; [**A**]), rod photoreceptors (recoverin; [**B**]), horizontal cells (calbindin; *arrows*) and their dendrites (*arrowheads*; [**C**]), cone (recoverin; [**D**]) and rod (PKC) bipolar cells' soma (*arrows*; [**E**]), their presynaptic connections (*arrowheads*; [**E**]) and axons (*arrows*) but not in postsynaptic connections (*arrowheads*; [**F**]), amacrine cells (syntaxin; [**G**]), ganglion cells (Brn-3a; [**H**]), and Müller cells (glutamine synthetase; [**I**]). *Scale bar*: 10 μm.

Investigative Ophthalmology & Visual Science

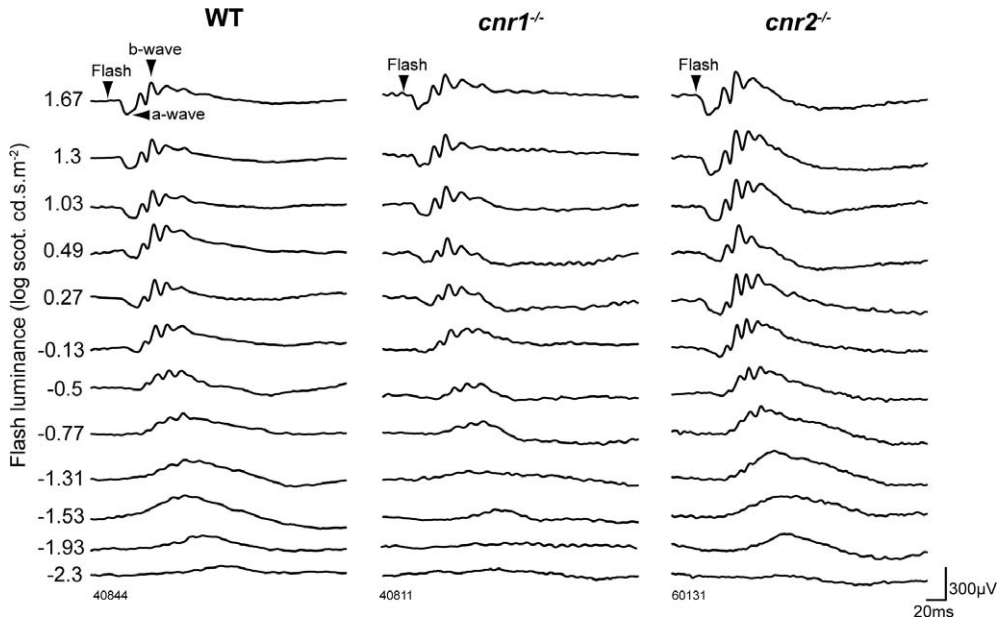

FIGURE 3. Example of scotopic ERGs in the different genotypes. Representative ERGs recorded in WT, *cnr1*$^{-/-}$, and *cnr2*$^{-/-}$ mice. The luminance-response function of each animal was established by presenting progressively brighter flashes (*bottom* to *top*) indicated to the *right* of the traces as the log luminance (scot cd-s/m^2).

Some amacrine cells showed also CB2R immunoreactivity at the membrane of the soma (Fig. 2G).

CB2R staining was detected in the GCL and was present in the ganglion cells' soma (Fig. 2H). CB2R was not expressed at the membrane of the Müller cells' soma or in their inner and outer processes (Fig. 2I).

The Dark-Adapted Retinal Function

We recorded dark-adapted retinal responses in WT, *cnr1*$^{-/-}$, and *cnr2*$^{-/-}$ mice at different light intensities. Representative examples of scotopic ERGs from WT, *cnr1*$^{-/-}$, and *cnr2*$^{-/-}$ mice are shown in Figure 3. The averaged a- and b-wave amplitudes are presented as a function of flash luminance in Figures 4A and 4B, respectively. A significant change in the a-wave amplitude was observed in *cnr2*$^{-/-}$ but not in *cnr1*$^{-/-}$ mice (repeated measures ANOVA with Dunnett post hoc test, for intensities 0.13 to 1.67 log scot cd-s/m^2, $P = 0.798$ for *cnr1*$^{-/-}$ and $P = 0.037$ for *cnr2*$^{-/-}$ mice). The amplitude of the b-wave (Fig. 4C) was not significantly altered in *cnr1*$^{-/-}$ or *cnr2*$^{-/-}$ mice. To better understand the change in the a-wave, the velocity-time profile was calculated at a saturating luminance (1.3 log scot cd-s/m^2). The averaged a-wave for all three groups is presented in Figure 4C. One can observe that the earliest part of the waveforms overlay and only separate in the latest segment. The averaged velocity-time profiles for all three groups are presented in Figure 4D. No differences were found in the accelerating (descending) portion of the curve (repeated measures ANOVA with Dunnett post hoc test from 0 to 7.4 ms). We confirmed those results by analyzing the a-wave amplitude at 7 ms[29] and found no significant differences between the groups. The deceleration (ascending) portion, however, showed significant changes between groups as *cnr2*$^{-/-}$ mice maintained higher velocities than WT animals (repeated measures ANOVA with Dunnett post hoc test from 7.4 to 15 ms, $P = 0.729$ for *cnr1*$^{-/-}$ and $P = 0.018$ for *cnr2*$^{-/-}$ mice). Fourier analysis was also performed on both a- and b-waves and revealed no other significant changes (data not shown).

Furthermore, the maximal ERG response evoked in scotopic conditions (the mixed rod-cone response) was also analyzed. The amplitude of the b-wave at maximal b-wave amplitude remained unchanged in all experimental groups (Table 2). No changes were observed in the luminance needed to evoke the maximal response in either group. No differences were observed in the latency of the a- and b-waves in both knockout (KO) groups, suggesting no involvement of CBRs in the kinetics of the response onset (data not shown).

The OPs were also analyzed, and representative examples of recordings for WT and *cnr2*$^{-/-}$ groups are presented in Figure 5A.The sum of all dark-adapted OPs was computed and compared. The averaged total amplitude is presented as a function of flash luminance in Figure 5B. We observed a tendency for the amplitude of the OPs to be larger between –0.13 to 1.30 log scot cd-s/m^2 in *cnr2*$^{-/-}$ than in WT animals. However, this tendency did not reach statistical significance. No changes were observed in the response of the *cnr1*$^{-/-}$ or *cnr2*$^{-/-}$ mice (repeated measures ANOVA, for intensities 0.13 to 1.67 log scot cd-s/m^2, $P = 0.345$). Fourier analysis was also performed and revealed no differences between the three genotypes (data not shown). No differences were observed in the latency of any of the analyzed OPs for either mice strain (results not shown).

The Light-Adapted Retinal Function

To evaluate the adaptation abilities of the retina, the ERG was recorded under photopic conditions at different time points. The averaged amplitude ± SEM of the photopic b-wave is displayed as a function of time in Figure 6. While the responses observed in *cnr1*$^{-/-}$ and WT mice are comparable, those in *cnr2*$^{-/-}$ mice have higher amplitudes at intermediate time points (one-way ANOVA, $P = 0.021$ and $P = 0.018$ for 10 and 15 minutes, respectively). The latency of the photopic b-wave did not vary across groups (data not shown). Light-adapted OPs were also analyzed and no significant changes were observed for any of the experimental groups (summed amplitude values; results not shown).

Investigative Ophthalmology & Visual Science

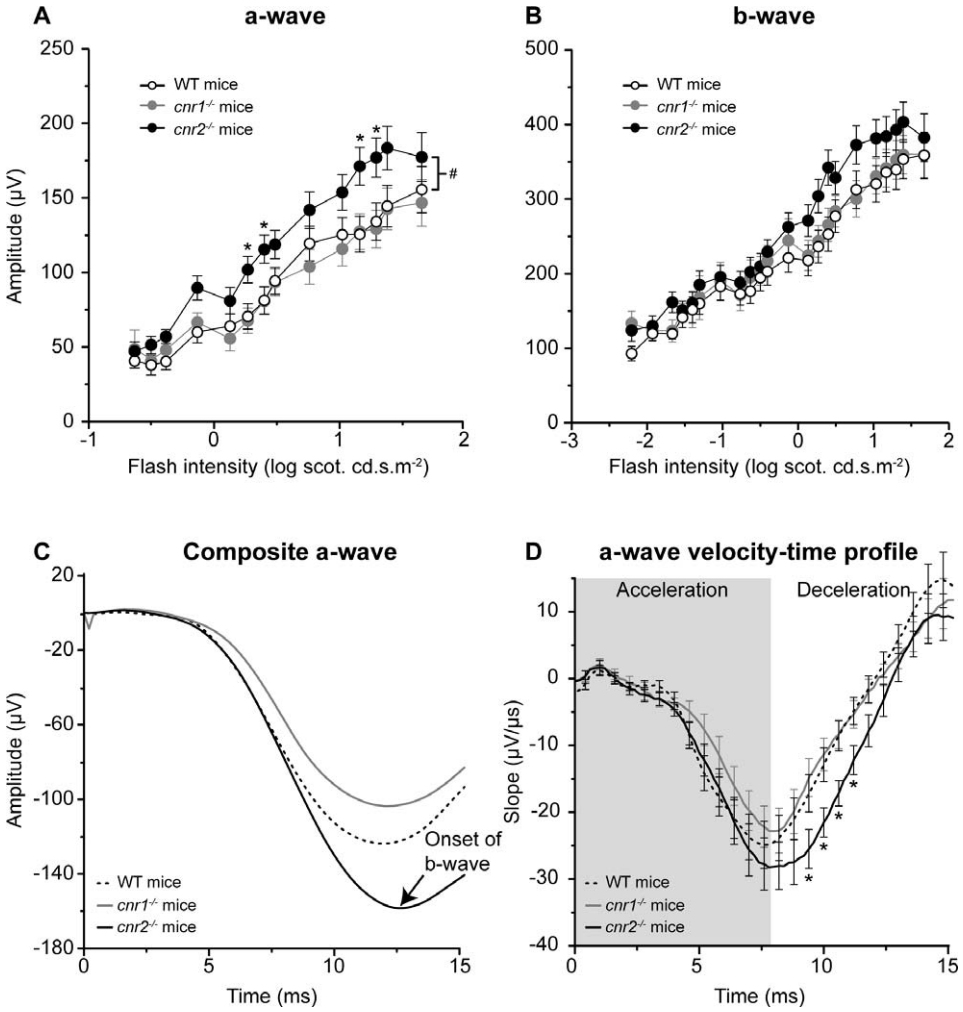

Figure 4. Amplitudes of scotopic ERG a- and b-waves plotted as a function of flash luminance. Scotopic ERG a-wave (**A**) and b-wave (**B**) amplitudes are displayed by genotype. The values are means ± SEM from all animals in each group (WT: *open circles*, $n = 20$; *cnr1*$^{-/-}$: *grey circles*, $n = 20$; *cnr2*$^{-/-}$: *closed circles*, $n = 18$; #repeated measures ANOVA, $P \leq 0.05$, *one-way ANOVA with Dunnett post hoc test, $P \leq 0.05$). (**C**) The averaged a-wave for each group is plotted as a function of time. (**D**) The velocity-time profile of the a-wave for each group displays differences between *cnr2*$^{-/-}$ and WT mice in the deceleration segment on the waveform (repeated measures ANOVA, $P \leq 0.05$; *one-way ANOVA with Dunnett post hoc test, $P \leq 0.05$).

Retinal Structure in *cnr1*$^{-/-}$ and *cnr2*$^{-/-}$ Mice

To ensure that there were no major structural changes in KO mice, we compared the basic retinal anatomy across groups by examining retinal layering and thickness. Figure 7A shows the typical retinal layering in all genotypes. First-look observations of the retinas showed no obvious changes in retinal structures. Then, the total retinal thickness (Fig. 7B), the thickness of each layer (Fig. 7C), and the number of cell rows for each nuclear layer (results not shown) were precisely measured. No significant differences were found for all parameters. The overall retinal layering was thus preserved in all genotypes. In addition, the distribution and morphology of retinal cells were compared for all genotypes to verify if they were affected. No obvious changes were observed in any retinal cell type for all genotypes (Figs. 8A–X).

Furthermore, we wanted to establish if the elimination of one receptor affected other elements of the eCB system. We measured the total amounts of CB2R, CB1R, synthesis enzymes NAPE-PLD and DAGLα, as well as degradative enzymes FAAH and MGL in the WT, *cnr1*$^{-/-}$, and *cnr2*$^{-/-}$ mice retina. No differences were found in the total amount of those proteins across groups (Figs. 9A–D).

Discussion

This study investigated the functional and anatomical consequences of knocking out CB1R or CB2R in the mouse retina.

Table 2. Group Data Reporting the Amplitudes of Mixed V_{max} as Well as the Light Intensities Evoking Them

	WT	*cnr1*$^{-/-}$	*cnr2*$^{-/-}$
Mixed V_{max}, μV	369 ± 29	371 ± 26	446 ± 22
Light luminance mixed V_{max}, log scot cd-s/m^2	1.27 ± 0.04	1.13 ± 0.05	1.06 ± 0.09

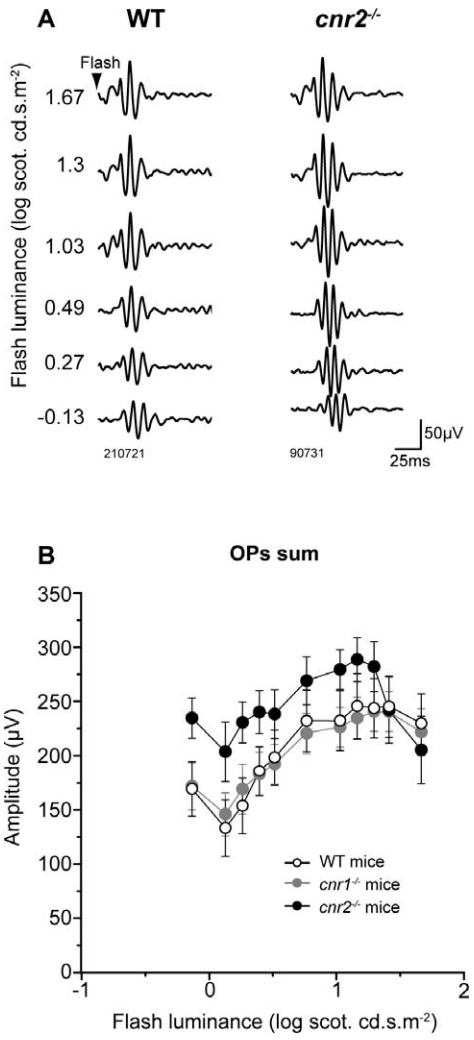

Figure 5. Example of scotopic OPs in the different groups. (**A**) Representative OPs recorded in WT and *cnr2*$^{-/-}$ mice. (**B**) The total sum of the amplitudes of all OPs is plotted as a function of flash luminance to compute the luminance-response function curve. The values are means ± SEM from all animals in each group (WT: *open circles*, $n = 17$; *cnr1*$^{-/-}$: *grey circles*, $n = 19$; *cnr2*$^{-/-}$: *closed circles*, $n = 12$).

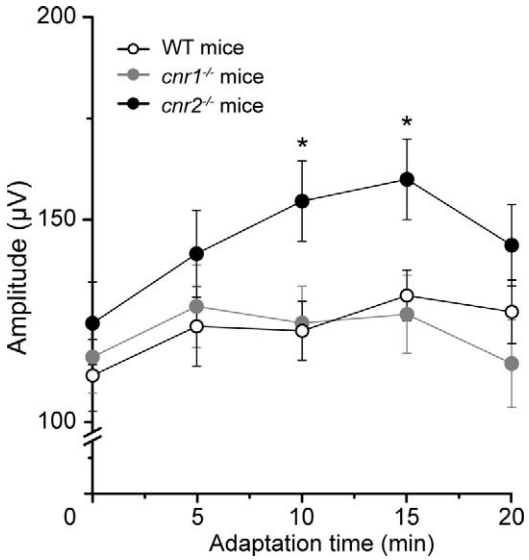

Figure 6. The amplitudes of photopic ERG b-wave are plotted as a function of time. Repeated ERGs were taken at different times and were used to evaluate the retina ability to adapt to light from a dark-adapted state. The *cnr2*$^{-/-}$ mice displayed significantly higher amplitudes at 10- and 15-minute time points (means ± SEM; WT: *open circles*, $n = 19$; *cnr1*$^{-/-}$: *grey circles*, $n = 18$; *cnr2*$^{-/-}$: *closed circles*, $n = 18$; *one-way ANOVA with Dunnett post hoc test, $P < 0.05$).

Using ERG, we showed that under scotopic conditions, the removal of CB1R did not change the response, while the absence of the CB2R affected the amplitude of the a-wave, without affecting the b-wave or amplitude and latency of the OPs. Under photopic conditions, removal of CB1R did not affect the retinal response, but the elimination of CB2R yielded a different light adaptation pattern. This study is the first evidence that CB2R affects global retinal function.

The CB2R Is Widely Distributed in the Mice Retina

The present results confirm the expression of CB2R in the rodent retina. To our knowledge, this study is the first to precisely localize CB2R in the mice retina by using an antibody controlled for specificity. Barutta et al.[22] have also used the same CB2R antibody and verified its specificity in *cnr2*$^{-/-}$ mice renal sections. Our results are in agreement with a study using RT-PCR and in situ hybridization, which shows that CB2R is present in the retinal ganglion cell layer, the INL, and the inner segments of photoreceptors cells.[16] A recent study has reported a similar distribution in the rat retina, with CB2R being localized in retinal pigmentary epithelium, inner photoreceptor segments, horizontal and amacrine cells, neurons in GCL, and fibers of the IPL.[17] Our results provided further confirmation of CB2R expression in mammalian retina. More specifically our data showed the presence of CB2R in cone and rod photoreceptors, horizontal cells, cone and rod bipolar cells, some amacrine cells, and ganglion cells.

CB1R Removal Does Not Affect the ERGs

Our data indicated that CB1R deletion does not have an impact on the retinal activity as measured with the ERG. This absence of functional changes observed in *cnr1*$^{-/-}$ mice was unexpected, given the wide distribution of CB1R expression in the rodent retina.[3,5,6] In addition, several authors[11–13] have reported that CBR activation differentially modulates calcium and potassium currents in rod and cone photoreceptors. These authors suggest that the net effect of CBR activation on calcium and potassium currents in rod photoreceptors would be a decrease in the light sensitivity. From these findings, we expected to observe increased amplitude in the a-wave in mice lacking CB1 receptor. As no effects were detected, this could indicate that the modulation of these currents by CB1R is too weak to be measured with the ERG.

The overall effect of CBR activation on cones is difficult to predict, as changes in ionic currents would lead to opposing outcomes.[13] Our data did not provide any more cues about this, since we did not observe an effect of CB1R removal on cone response.

Electroretinograms reflect essentially the activity of photoreceptors and bipolar cells. Consequently, our data do not preclude a role for CB1R in the response of other retinal neurons such as horizontal, amacrine, and ganglion cells. The latter is further supported by several studies demonstrating that CB1R activity modulates the excitability of amacrine and ganglion cells.[8,9,30] Nevertheless, altogether our results suggest

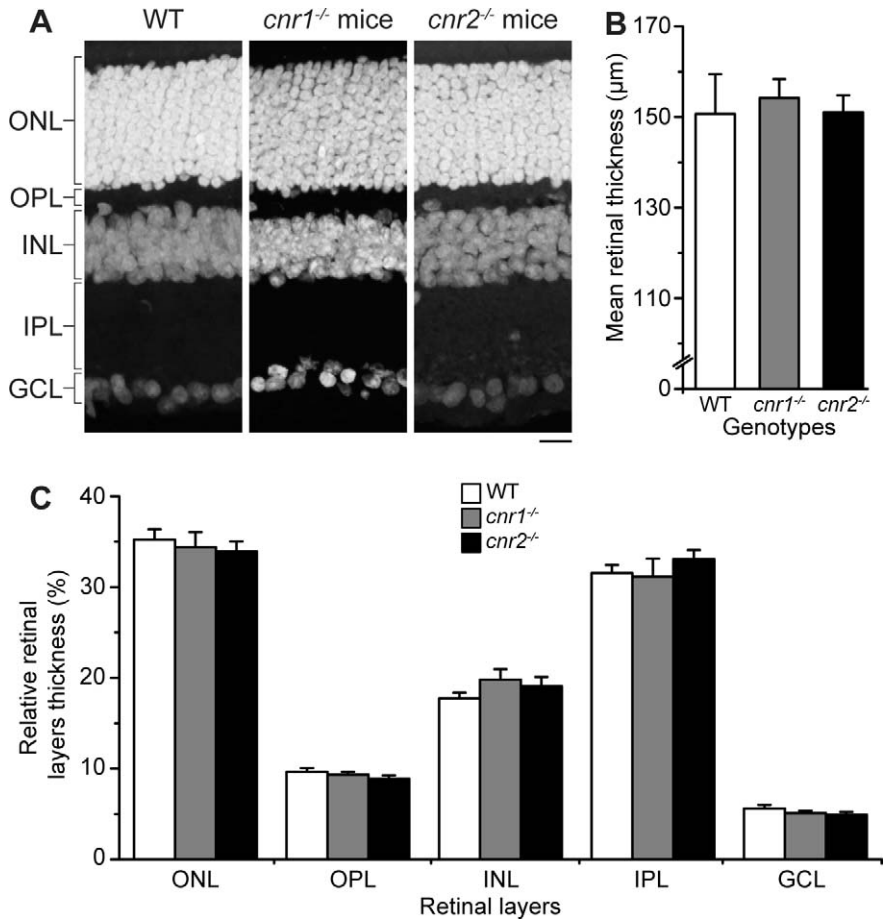

Figure 7. Deletion of *cnr1* or *cnr2* does not change retinal morphology. (**A**) Nuclei staining of retinas of WT, *cnr1*$^{-/-}$, and *cnr2*$^{-/-}$ mice with Sytox. Normal retinal layer structures were preserved in all mice. *Scale bar*: 20 µm. (**B**) Total thickness calculated from ONL-GCL in the three genotypes. (**C**) Mean thickness of each retinal layer in the three genotypes. *White*, *grey*, and *black bars* correspond to the WT, *cnr1*$^{-/-}$, and *cnr2*$^{-/-}$ mice, respectively.

that the absence of CB1R does not affect the global response of the retina. However, this receptor could still affect other visual structures, as we[31] recently have reported that CB1R exerts a regulatory action on the neurovascular coupling and functional organization of the mice visual cortex along the azimuth axis.

Effect of CB2R Removal on the ERGs

Under scotopic conditions, our data indicated that the amplitude of the a-wave is larger in *cnr2*$^{-/-}$ than in WT mice at several intensities. The a-wave is thought to originate from photoreceptors; hence, this effect may reflect the consequences of CB2R removal on these cells. As mentioned earlier in the introduction, the activation of CBRs by the administration of an agonist can decrease the sensitivity of rod photoreceptors.[13] Provided that we report no changes in the a-wave of *cnr1*$^{-/-}$ mice and an increased a-wave in *cnr2*$^{-/-}$ mice, we suggest that the alteration of rod sensitivity reported in Straiker and Sullivan[13] could be mediated by CB2R rather than CB1R. Analysis of the velocity-time profile at saturating luminance revealed no differences in the accelerating segment of the a-wave (the leading edge) between groups. However, this analysis indicated that the *cnr2*$^{-/-}$ mice maintained higher velocities than their WT counterparts in the decelerating segment of the a-wave. One may propose that CB2R deletion decreases the postreceptoral contribution to the a-wave. This hypothesis is unlikely as it has been shown that the a-wave profile is not modified by the pharmacologic elimination of the b-wave at saturating intensities.[32] Since it has been shown that the decelerating segment could be caused by the recovery of the a-wave,[33] our results may indicate that photoreceptors recuperate more slowly in *cnr2*$^{-/-}$ mice.

Anatomical studies showed that CB2R was expressed in the bipolar cells of mice (this article and Lu et al.[16]). Moreover, Yazulla et al.[14] have demonstrated that CBRs modulate potassium currents in retinal bipolar cells. Based on these findings and given that bipolar cells contribute, in part, to the genesis of the b-wave, one can expect that CB2R elimination will affect the b-wave amplitude and/or latency. Our present results showed only a trend in which all the b-wave data points have higher amplitude in *cnr2*$^{-/-}$ than in WT or *cnr1*$^{-/-}$ mice. No such tendencies were observed for the b-wave latency. These results indicate a limited effect of CB2R on the b-wave, while the effect on the a-wave is larger.

Under photopic conditions, an enhanced b-wave was observed at intermediate recording time points (10 and 15 minutes) in *cnr2*$^{-/-}$ mice. Among the roles most commonly attributed to cannabinoid receptors are adaptive mechanisms such as long-term-depression[34–36] and downregulation of synaptic release[11] in the visual system and elsewhere. Thus, these results suggest that CBRs are likely to be involved in mechanisms subtending retinal adaptation.

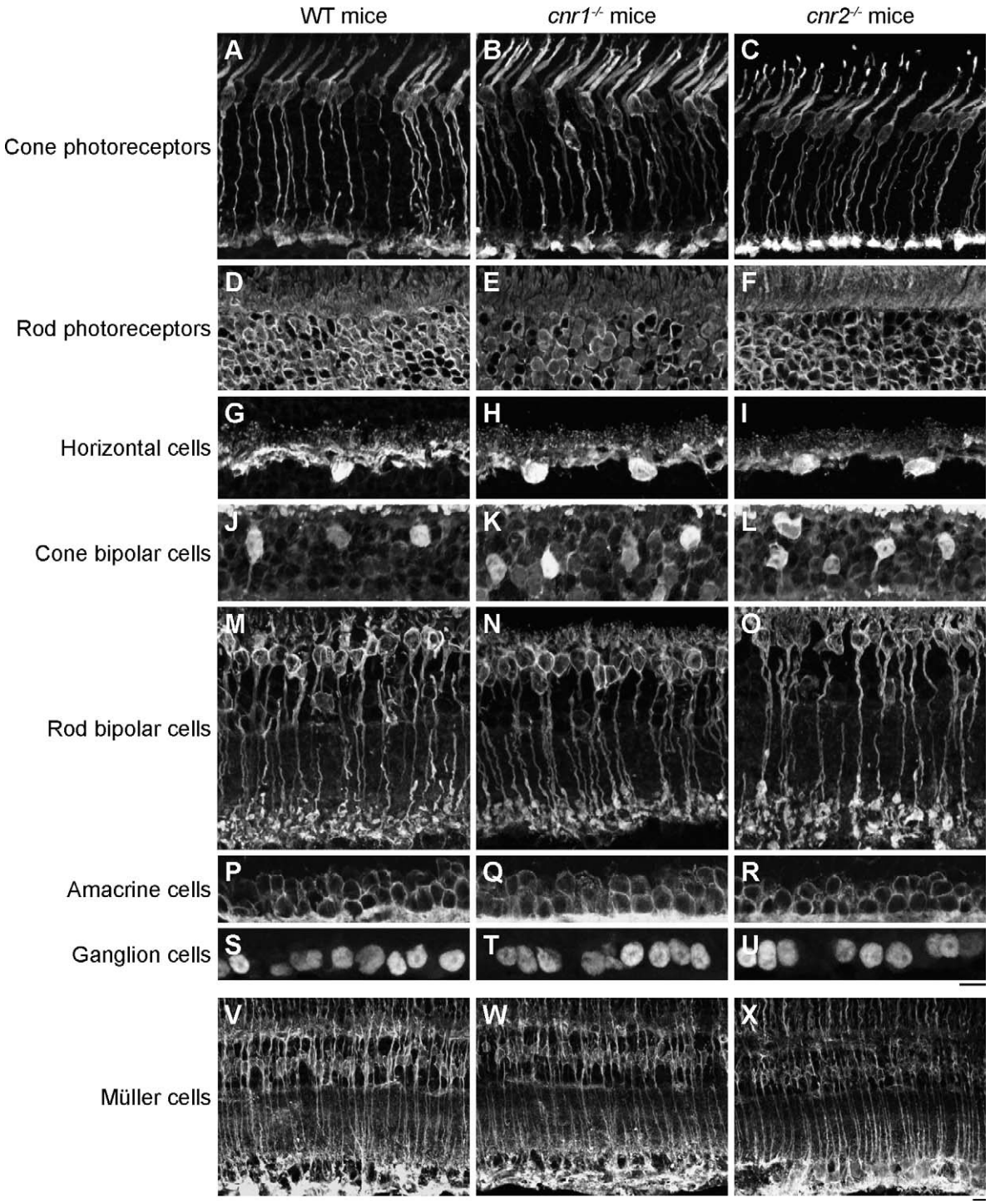

Figure 8. Absence of CB1R or CB2R does not produce any obvious changes in the distribution and morphology of cone photoreceptors (mouse cone-arrestin; [**A–C**]), rod photoreceptors (recoverin; [**D–F**]), horizontal cells (calbindin; [**G–I**]), cone bipolar cells (recoverin; [**J–L**]), rod bipolar cells (PKC; [**M–O**]), amacrine cells (HPC; [**P–R**]), ganglion cells (Brn-3a; [**S–U**]), and Müller cells (glutamine synthetase; [**V–X**]) in WT, *cnr1*$^{-/-}$, and *cnr2*$^{-/-}$ mice. Normal morphology and distribution of every retinal cell types were preserved in all mice. *Scale bars*: 10 μm.

We showed that functional changes observed in *cnr1*$^{-/-}$ and *cnr2*$^{-/-}$ mice are not due to abnormal retinal cell distribution or compensation of the eCB system activity. Previous studies have shown that the eCB system interacts with GABA, glutamate, and dopamine systems.[37–40] For example, CB1R agonists stimulate dopamine release from the guinea pig retina.[37] Hence, the changes in retinal response in *cnr2*$^{-/-}$ mice, and/or lack thereof in *cnr1*$^{-/-}$ mice, could be partly due to compensation mechanisms in GABA, glutamate, or dopamine systems.

In conclusion, this study demonstrated that CB2R is expressed in several cell types in the mice retina. Our results also suggest that CB1R and CB2R contribute differently to visual functions: CB1R does not seem to be involved in global retinal responses, while CB2R appears to be implicated in rod and cone sensitivity and light adaptation.

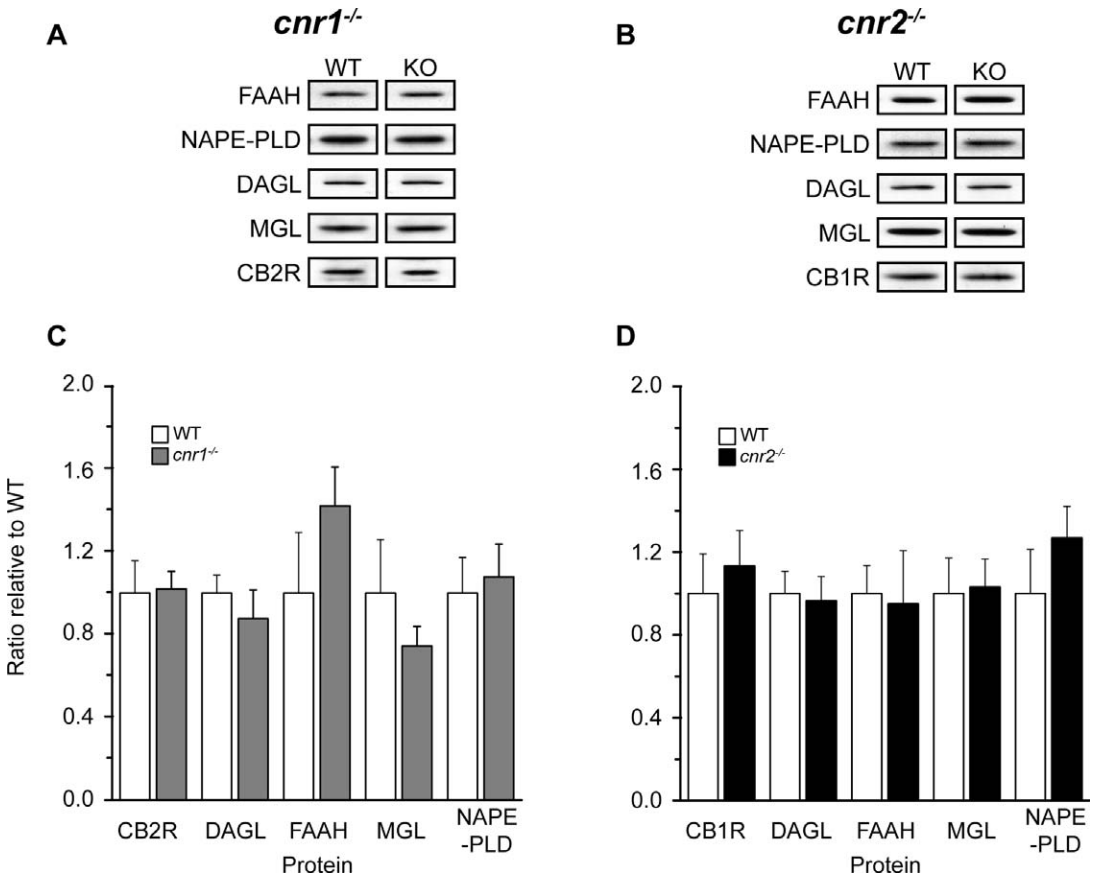

Figure 9. Total retinal concentration of proteins from the eCB system. (**A**, **B**) Representative examples of FAAH, NAPE-PLD, DAGLα, MGL, CB1R, and CB2R expression in WT, *cnr1*$^{-/-}$, and *cnr2*$^{-/-}$ mice retina lysate. (**C**, **D**) Averaged ratio ± SEM relative to WT of FAAH, NAPE-PLD, DAGLα, MGL, CB1R, and CB2R expression in WT (*white*), *cnr1*$^{-/-}$ (*grey*), and *cnr2*$^{-/-}$ (*black*) mice. Specific bands were seen at around 53 kDa for CB1R, 45 kDa for CB2R, 120 kDa for DAGLα, 66 kDa for FAAH, 37 kDa for MGL, and 46 kDa for NAPE-PLD.

Acknowledgments

We thank Pierre Lachapelle (McGill University, Montréal, Quebec, Canada) for his constructive comments on this manuscript, and Vasil Diaconu (University of Montreal, Montréal, Quebec, Canada) for light measurements. We thank the Mary D. Allen Laboratory for Vision Research, Doheny Eye Institute, and Cheryl M. Craft for generously supplying the antibody against cone arrestin. We also thank Alexandra Gagné and Sébastien Thomas for their excellent assistance.

Supported by a joint Fonds de recherche du Québec-Santé (FRQS) Vision Network grant – Fondation des maladies de l'oeil and Canadian Institutes of Health Research (CIHR) Grant MOP 130337 (J-FB and CC), by NSERC Grant 194670-2009 (CC), and by CIHR Grant MOP 177796 and Natural Sciences and Engineering Research Council of Canada (NSERC) Grant 311892-2010 (J-FB). Also supported by a CIHR-E.A. Baker Foundation studentship (NZ), a Réseau FRQS de recherche en santé de la vision studentship (BC), and a Chercheur-Boursier Junior 2 from the FRQS (J-FB).

Disclosure: **B. Cécyre**, None; **N. Zabouri**, None; **F. Huppé-Gourgues**, None; **J.-F. Bouchard**, None; **C. Casanova**, None

References

1. Straiker A, Maguire G, Mackie K, Lindsey J. Localization of cannabinoid CB1 receptors in the human anterior eye and retina. *Invest Ophthalmol Vis Sci*. 1999;40:2442–2448.
2. Straiker A, Stella N, Piomelli D, Mackie K, Karten HJ, Maguire G. Cannabinoid CB1 receptors and ligands in vertebrate retina: localization and function of an endogenous signaling system. *Proc Natl Acad Sci U S A*. 1999;96:14565–14570.
3. Yazulla S, Studholme KM, McIntosh HH, Deutsch DG. Immunocytochemical localization of cannabinoid CB1 receptor and fatty acid amide hydrolase in rat retina. *J Comp Neurol*. 1999;415:80–90.
4. Bouskila J, Burke MW, Zabouri N, Casanova C, Ptito M, Bouchard JF. Expression and localization of the cannabinoid receptor type 1 and the enzyme fatty acid amide hydrolase in the retina of vervet monkeys. *Neuroscience*. 2012;202:117–130.
5. Hu SS, Arnold A, Hutchens JM, et al. Architecture of cannabinoid signaling in mouse retina. *J Comp Neurol*. 2010;518:3848–3866.
6. Zabouri N, Bouchard JF, Casanova C. Cannabinoid receptor type 1 expression during postnatal development of the rat retina. *J Comp Neurol*. 2011;519:1258–1280.
7. Leonelli M, Britto LR, Chaves GP, Torrao AS. Developmental expression of cannabinoid receptors in the chick retinotectal system. *Brain Res Dev Brain Res*. 2005;156:176–182.
8. Warrier A, Wilson M. Endocannabinoid signaling regulates spontaneous transmitter release from embryonic retinal amacrine cells. *Vis Neurosci*. 2007;24:25–35.
9. Lalonde MR, Jollimore CA, Stevens K, Barnes S, Kelly ME. Cannabinoid receptor-mediated inhibition of calcium signaling in rat retinal ganglion cells. *Mol Vis*. 2006;12:1160–1166.
10. Yazulla S. Endocannabinoids in the retina: from marijuana to neuroprotection. *Prog Retin Eye Res*. 2008;27:501–526.

11. Fan SF, Yazulla S. Retrograde endocannabinoid inhibition of goldfish retinal cones is mediated by 2-arachidonoyl glycerol. *Vis Neurosci*. 2007;24:257–267.
12. Fan SF, Yazulla S. Biphasic modulation of voltage-dependent currents of retinal cones by cannabinoid CB1 receptor agonist WIN 55212-2. *Vis Neurosci*. 2003;20:177–188.
13. Straiker A, Sullivan JM. Cannabinoid receptor activation differentially modulates ion channels in photoreceptors of the tiger salamander. *J Neurophysiol*. 2003;89:2647–2654.
14. Yazulla S, Studholme KM, McIntosh HH, Fan SF. Cannabinoid receptors on goldfish retinal bipolar cells: electron-microscope immunocytochemistry and whole-cell recordings. *Vis Neurosci*. 2000;17:391–401.
15. Atwood BK, Mackie K. CB2: a cannabinoid receptor with an identity crisis. *Br J Pharmacol*. 2010;160:467–479.
16. Lu Q, Straiker A, Lu Q, Maguire G. Expression of CB2 cannabinoid receptor mRNA in adult rat retina. *Vis Neurosci*. 2000;17:91–95.
17. Lopez EM, Tagliaferro P, Onaivi ES, Lopez-Costa JJ. Distribution of CB2 cannabinoid receptor in adult rat retina. *Synapse*. 2011;65:388–392.
18. de Sousa Abreu R, Penalva LO, Marcotte EM, Vogel C. Global signatures of protein and mRNA expression levels. *Mol Biosyst*. 2009;5:1512–1526.
19. Nikonov SS, Brown BM, Davis JA, et al. Mouse cones require an arrestin for normal inactivation of phototransduction. *Neuron*. 2008;59:462–474.
20. Zhu X, Brown B, Li A, Mears AJ, Swaroop A, Craft CM. GRK1-dependent phosphorylation of S and M opsins and their binding to cone arrestin during cone phototransduction in the mouse retina. *J Neurosci*. 2003;23:6152–6160.
21. Zhu X, Li A, Brown B, Weiss ER, Osawa S, Craft CM. Mouse cone arrestin expression pattern: light induced translocation in cone photoreceptors. *Mol Vis*. 2002;8:462–471.
22. Barutta F, Piscitelli F, Pinach S, et al. Protective role of cannabinoid receptor type 2 in a mouse model of diabetic nephropathy. *Diabetes*. 2011;60:2386–2396.
23. Schindelin J, Arganda-Carreras I, Frise E, et al. Fiji: an open-source platform for biological-image analysis. *Nat Methods*. 2012;9:676–682.
24. Luisier F, Blu T. SURE-LET multichannel image denoising: interscale orthonormal wavelet thresholding. *IEEE Trans Image Processing*. 2008;17:482–492.
25. Plaziac C, Lachapelle P, Casanova C. Effects of methanol on the retinal function of juvenile rats. *Neurotoxicology*. 2003;24:255–260.
26. Sagdullaev BT, DeMarco PJ, McCall MA. Improved contact lens electrode for corneal ERG recordings in mice. *Doc Ophthalmol*. 2004;108:181–184.
27. Marmor MF, Fulton AB, Holder GE, et al. ISCEV Standard for full-field clinical electroretinography (2008 update). *Doc Ophthalmol*. 2009;118:69–77.
28. Weymouth AE, Vingrys AJ. Rodent electroretinography: methods for extraction and interpretation of rod and cone responses. *Prog Retin Eye Res*. 2008;27:1–44.
29. Heckenlively JR, Arden GB. *Principles and Practice of Clinical Electrophysiology of Vision*. 2nd ed. Cambridge, MA: MIT Press; 2006.
30. Middleton T, Protti D. Cannabinoids modulate spontaneous synaptic activity in retinal ganglion cells. *Vis Neurosci*. 2011;28:393–402.
31. Abbas Farishta R, Robert C, Vanni MP, Minville K, Bouchard JF, Casanova C. *Effects of Cannabinoid CB1 Receptor on Hemodynamic Responses and Functional Organization of the Primary Visual Cortex: 2010 Neuroscience Meeting Planner*. San Diego, CA: Society for Neuroscience; 2010.
32. Lei B. Rod-driven OFF pathway responses in the distal retina: dark-adapted flicker electroretinogram in mouse. *PLoS One*. 2012;7:e43856.
33. Kang Derwent JJ, Linsenmeier RA. Intraretinal analysis of the a-wave of the electroretinogram (ERG) in dark-adapted intact cat retina. *Vis Neurosci*. 2001;18:353–363.
34. Liu CH, Heynen AJ, Shuler MG, Bear MF. Cannabinoid receptor blockade reveals parallel plasticity mechanisms in different layers of mouse visual cortex. *Neuron*. 2008;58:340–345.
35. Huang Y, Yasuda H, Sarihi A, Tsumoto T. Roles of endocannabinoids in heterosynaptic long-term depression of excitatory synaptic transmission in visual cortex of young mice. *J Neurosci*. 2008;28:7074–7083.
36. Sjostrom PJ, Turrigiano GG, Nelson SB. Neocortical LTD via coincident activation of presynaptic NMDA and cannabinoid receptors. *Neuron*. 2003;39:641–654.
37. Schlicker E, Timm J, Gothert M. Cannabinoid receptor-mediated inhibition of dopamine release in the retina. *Naunyn Schmiedebergs Arch Pharmacol*. 1996;354:791–795.
38. Romero J, de Miguel R, Ramos JA, Fernandez-Ruiz JJ. The activation of cannabinoid receptors in striatonigral GABAergic neurons inhibited GABA uptake. *Life Sci*. 1998;62:351–363.
39. Chan PK, Chan SC, Yung WH. Presynaptic inhibition of GABAergic inputs to rat substantia nigra pars reticulata neurones by a cannabinoid agonist. *Neuroreport*. 1998;9:671–675.
40. Shen M, Piser TM, Seybold VS, Thayer SA. Cannabinoid receptor agonists inhibit glutamatergic synaptic transmission in rat hippocampal cultures. *J Neurosci*. 1996;16:4322–4334.

Investigative Ophthalmology & Visual Science